and

$$k = \frac{\epsilon - \epsilon_o}{\epsilon + \epsilon_o}.$$

Acknowledgment

The authors would like to thank C. E. Nelson, General Electric Company, for helpful discussions, and G. Capraro, Rome Air Development Center, for his assistance in computation.

References

[1] R. F. Harrington, *Field Computation by Moment Methods*. New York: Macmillan, 1968.
[2] B. J. Strait and A. T. Adams, "Analysis and design of wire antennas with application to EMC," *IEEE Trans. Electromagn. Compat.*, vol. EMC-12, pp. 45–54, May 1970.
[3] R. F. Harrington, "Matrix methods for field problems," *Proc. IEEE*, vol. 55, pp. 136–149, Feb. 1967.
[4] A. Farrar and A. T. Adams, "Computation of lumped microstrip capacities by matrix methods—Rectangular sections and end effect," *IEEE Trans. Microwave Theory Tech.* (Corresp.), vol. MTT-19, pp. 495–497, May 1971.
[5] ——, "Computation of static capacitance data for single, double, and triple microstrip," in *1970 G-MTT Symp. Dig.*, pp. 257–261.
[6] H. Stinehelfer, "Strip transmission lines," *Microwave J.*, pp. 71–72, Feb. 1969.
[7] A. A. Oliner, "Equivalent circuit for discontinuities in balanced strip transmission line," *IRE Trans. Microwave Theory Tech. (Special Issue: Symposium on Microwave Strip Circuits)*, vol. MTT-3, pp. 134–143, Mar. 1955.
[8] J. R. Whinnery and H. W. Jamieson, "Equivalent circuit for discontinuities in transmission lines," *Proc. IRE*, vol. 32, pp. 98–114, Feb. 1944.
[9] D. K. Reitan, "Accurate determination of the capacitance of rectangular parallel plate capacitors," *J. Appl. Phys.*, vol. 30, no. 2, pp. 172–176, Feb. 1959.
[10] A. T. Adams and J. R. Mautz, "Computer solution of electrostatic problems by matrix inversion," in *Proc. 1969 Nat. Electronics Conf.*, pp. 198–201.
[11] E. Durand, *Electrostatique* I—*Les Distributions*. Paris, France: Masson et Cie, 1964, pp. 243–246.
[12] P. Silvester, "TEM wave properties of microstrip transmission line," *Proc. Inst. Elec. Eng.*, vol. 115, no. 1, pp. 43–48, Jan. 1968.
[13] Y. M. Hill, N. O. Reckord, and D. R. Winner, "A general method for obtaining impedance and coupling characteristics of practical microstrip and triplate transmission line configurations," *IBM J. Res. Develop.*, vol. 13, no. 3, pp. 314–322, May 1969.

Capacitance of Parallel Rectangular Plates Separated by a Dielectric Sheet

PETER BENEDEK, STUDENT MEMBER, IEEE, AND P. SILVESTER, MEMBER, IEEE

Abstract—**To determine the capacitance between two rectangular parallel plates separated by a dielectric sheet, the charge distribution on the plates is formulated in terms of a Fredholm integral equation of the first kind. This equation is solved numerically by a projective method using polynomial approximants. The resulting capacitance values are given in normalized graphical form, permitting capacitance determination for any practical values of dielectric constant and geometric parameters to within a few percent.**

Introduction

IN RECENT YEARS a substantial amount of literature has become available for microstriplike and related structures. But even with the increased use of integrated circuits, there appears to be very little data for finite plates on dielectric substrates. Reitan [1] obtained the capacitance of two parallel square plates *in vacuo* using the method of subareas. Harrington [2] solved the same problem using a closely related projection method. Adams and Mautz [3] found the capacitance of a rectangular dielectric loaded capacitor by the point-matching method and introduced special matrix elements to take care of the air–dielectric interface. Farrar and Adams [4] obtained, very recently, the capacitance of a rectangular section of a microstrip line by the method of moments with pulse-expansion functions and impulsive weights. They calculate the potential due to a uniformly charged rectangular plate *in vacuo* and then generate the Green's function as an infinite series of images.

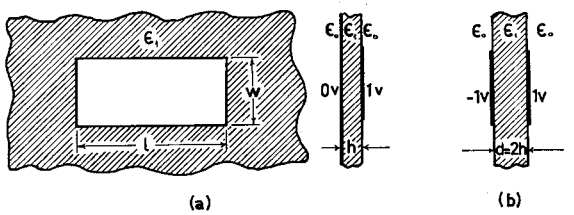

Fig. 1. (a) Rectangular metal plate on a metal-backed dielectric substrate. (b) Parallel plate problem, equivalent to (a).

This paper takes a different approach to the static capacitance for rectangular thin plates on a metal-backed dielectric substrate, as shown in Fig. 1(a). To facilitate the analysis, the equivalent problem, shown in Fig. 1(b), is considered. It is well known that the electrostatic behavior of this configuration is governed by Poisson's equation subject to Dirichlet boundary condi-

Manuscript received August 3, 1971; revised November 29, 1971. This work was supported in part by the Communications Research Centre and by the National Research Council of Canada.

The authors are with the Department of Electrical Engineering, McGill University, Montreal, Que., Canada.

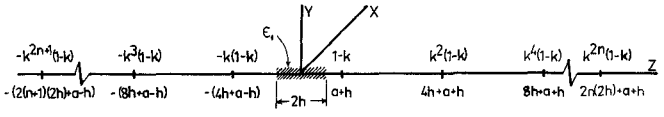

Fig. 2. Image representation valid in the dielectric region for a unit point charge near a dielectric sheet.

tions at infinity, i.e.,

$$-\nabla^2\phi(x) = \rho(x)/\epsilon \tag{1}$$

$$\phi(x) = 0, \qquad \text{for } |x| = \infty \tag{2}$$

where ϕ is the electrostatic potential, ρ is some charge-density distribution, and x denotes any space point.

This, however, being a three-dimensional exterior problem, is not well suited to be approached from a differential equation point of view. Instead, the equivalent integral equation must be obtained via the Green's function technique. It can be shown [5] that the integral equation is of the form

$$\phi(x) = \int_R g(x;\xi)\sigma(\xi)\,d\xi \tag{3}$$

where $g(x;\xi)$ is the appropriate Green's function. The indicated integration is over the whole space, but in fact it needs to be performed only where the charge density $\sigma(\xi)$ on the plates is not zero.

The Green's Function

It is well known that the three-dimensional Green's function for the Laplacian operator in a homogeneous medium is

$$g(x;\xi) = \frac{1}{4\pi\epsilon|x-\xi|}. \tag{4}$$

In the present context, $g(x;\xi)$ represents the electrostatic potential at a point x due to a unit point charge at ξ.

Silvester [6] used the method of images to obtain the Green's function for the two-dimensional microstrip problem. He showed that for a point charge at a distance a from a dielectric sheet of thickness $2h$, the image representation valid in the dielectric region is as shown in Fig. 2. This representation is equally valid for three-dimensional problems. Therefore, the potential at a point (x, y, z) with $-h \le z \le h$ due to a unit point charge is

$$V(x,y,z) = \frac{1-k}{4\pi\epsilon_1}\sum_{n=0}^{\infty} k^{2n} \cdot \frac{1}{\sqrt{(x-x_0)^2+(y-y_0)^2+[z-(4n+1)h-a]^2}} - \frac{k(1-k)}{4\pi\epsilon_1}\sum_{n=0}^{\infty} k^{2n} \cdot \frac{1}{\sqrt{(x-x_0)^2+(y-y_0)^2+[z+(4n+3)h+a]^2}} \tag{5}$$

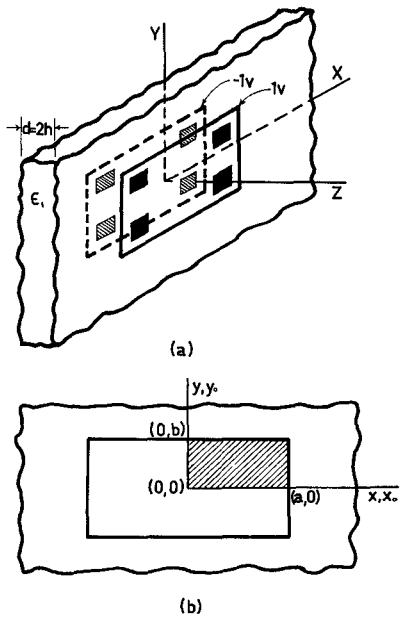

Fig. 3. (a) Eight-way symmetry for the parallel plates. (b) Positive quadrant of top plate to be used with Green's function in (7).

where $k = (\epsilon_0 - \epsilon_1)/(\epsilon_0 + \epsilon_1)$ is the image coefficient. For a thin plate $a = 0$, so that the potential in the $z = h$ plane is given by

$$V(x,y) = \frac{1-k}{4\pi\epsilon_1}\sum_{n=0}^{\infty} k^{2n} \cdot \frac{1}{\sqrt{(4nh)^2+(x-x_0)^2+(y-y_0)^2}} - \frac{k(1-k)}{4\pi\epsilon_1}\sum_{n=0}^{\infty} k^{2n} \cdot \frac{1}{\sqrt{[4(n+1)h]^2+(x-x_0)^2+(y-y_0)^2}}. \tag{6}$$

Now using the inherent eight-way symmetry in the configuration, as shown in Fig. 3(a), the Green's function is

$$g(x,y;x_0,y_0) = \frac{1}{2\pi(\epsilon_0+\epsilon_1)h}\left[f(0) - (1-k)\sum_{n=1}^{\infty} k^{n-1}f(n)\right] \tag{7}$$

where

$$f(n) = \left[(2n)^2 + \left(\frac{x-x_0}{h}\right)^2 + \left(\frac{y-y_0}{h}\right)^2\right]^{-1/2} + \left[(2n)^2 + \left(\frac{x+x_0}{h}\right)^2 + \left(\frac{y-y_0}{h}\right)^2\right]^{-1/2} + \left[(2n)^2 + \left(\frac{x-x_0}{h}\right)^2 + \left(\frac{y+y_0}{h}\right)^2\right]^{-1/2} + \left[(2n)^2 + \left(\frac{x+x_0}{h}\right)^2 + \left(\frac{y+y_0}{h}\right)^2\right]^{-1/2}. \tag{8}$$

Using Green's function in (7), with all the image points built into it, only the positive quadrant of the top plate needs to be considered, as shown in Fig. 3(b). A similar Green's function, containing only half the terms of (6), has recently been obtained by Patel [7] for the case when the ground plane is at infinity.

Solution of the Integral Equation by Galerkin's Method

Substituting Green's function from (7) into the integral equation (3) and integrating over one quadrant as required by Fig. 3(b),

$$\int_{y=0}^{b}\int_{x=0}^{a} g(x, y; x_0, y_0)\sigma(x, y)\,dxdy = \phi(x_0, y_0). \quad (9)$$

Note that the three-dimensional boundary-value problem has been reduced to a two-dimensional integral equation. The question asked by (9) is, *"What charge distribution $\sigma(x, y)$ is required on the plate to produce some given potential on it?"*

Let the quadrant under consideration be discretized into M smaller rectangles of arbitrary shapes, and define the solution $\sigma(x, y)$ and given potential $\phi(x_0, y_0)$ in the ith subregion as $\sigma^i(x, y)$ and $\phi^i(x_0, y_0)$, respectively. Both σ^i and ϕ^i are taken to be zero outside the ith subregion. Therefore,

$$\sigma(x, y) = \sum_{i=0}^{M} \sigma^i(x, y) \quad (10)$$

$$\phi(x_0, y_0) = \sum_{i=1}^{M} \phi^i(x_0, y_0). \quad (11)$$

In the ith subregion expand $\sigma^i(x, y)$ in terms of an n-term linearly independent set of functions $\{v_j^i(x, y), j=1, 2, \cdots, n\}$, i.e.,

$$\sigma^i(x, y) = \sum_{j=1}^{n} c_j^i v_j^i(x, y). \quad (12)$$

Substituting (10)–(12) into (9) and defining

$$G_j^i(x_0, y_0) = \int_{y=0}^{b}\int_{x=0}^{a} g(x, y; x_0, y_0)v_j^i(x, y)\,dxdy \quad (13)$$

we obtain

$$\sum_{i=1}^{M}\sum_{j=1}^{n} c_j^i G_j^i(x_0, y_0) = \sum_{i=1}^{M} \phi^i(x_0, y_0). \quad (14)$$

In the kth subregion, introduce a set of n linearly independent weight functions $t_l^k(x_0, y_0)$ for projection purposes. By the Galerkin–Petrov method [10] it is required that both sides of (14) be projected onto space spanned by a set of weight functions, such as $\{t_l^k(x_0, y_0)\}$. In this process note that the inner product $(\phi^i(x_0, y_0), t_l^k(x_0, y_0)) = 0$ when $i \neq k$, so that the result of the projection is

$$\sum_{i=1}^{M}\sum_{j=1}^{n} c_j^i(G_j^i(x_0, y_0), t_l^k(x_0, y_0)) = (\phi^k(x_0, y_0), t_l^k(x_0, y_0)),$$

$$\text{with } k = 1, 2, \cdots, M \text{ and } l = 1, 2, \cdots, n. \quad (15)$$

This is an $Mn \times Mn$ matrix equation that can be solved for the unknown coefficients c_j^i by any standard technique. Once the c_j^i are known the charge distribution is readily found. Now the total charge on the top plate can be obtained, and the normalized capacitance with respect to the bottom plate at -1 V is determined as

$$C = \frac{q_t d}{2\epsilon_0 A} \quad (16)$$

where

- q_t total charge on the top plate;
- A area of the top plate;
- d $= 2h =$ spacing between the top and bottom plates;
- ϵ_0 $= 8.85 \times 10^{-12}$ F/m.

Numerical Evaluation of the Inner Products

Consider the typical inner product

$$(G_j^i(x_0, y_0), t_l^k(x_0, y_0)) = \int\!\!\int_{\substack{k\text{th}\\ \text{region}}} \int\!\!\int_{\substack{i\text{th}\\ \text{region}}} g(x, y; x_0, y_0) \cdot v_j^i(x, y)t_l^k(x_0, y_0)\,dxdydx_0dy_0 \quad (17)$$

where $g(x, y; x_0, y_0)$ is given in (7). Three cases arise that need to be examined in some detail.

To perform the integration indicated in (17) when the integrand contains no singularities, a four-dimensional Cartesian product rule is used. This involves considering (17) as an iterated integral and using a Guassian integration formula in each coordinate direction [8]. Using a three-point Gaussian quadrature formula in each direction yields 81 quadrature points for the four-dimensional region. Although in principle fewer points may be sufficient to integrate four-dimensional complete polynomials of the fifth degree (i.e., all polynomials $x_1^i x_2^j x_3^k x_4^l$ such that $i+j+k+l \leq 5$), the extra points are not wasted as these permit the exact integration of all polynomials $x_1^i x_2^j x_3^k x_4^l$ such that i, j, k, and $l \leq 5$.

The second case that it is necessary to consider arises when $i = k$ in (17). In this case the Green's function contains a singularity. The integral (17) is of the form

$$l_1 = \int_{y_0=c}^{d}\int_{x_0=a}^{b}\int_{y=c}^{d}\int_{x=a}^{b} \cdot \frac{v(x, y)t(x_0, y_0)}{\sqrt{(x - x_0)^2 + (y - y_0)^2}}\,dxdydx_0dy_0. \quad (18)$$

This integration is once again over a hypercube, but here there is a singularity at $x = x_0$ and $y = y_0$. However, performing two coordinate transformations these singularity regions can be very conveniently reduced to a point. First, let the order of integration in (18) be changed to

$$l_1 = \int_{y_0=c}^{d}\int_{y=c}^{d}\left[\int_{x_0=a}^{b}\int_{x=a}^{b} \cdot \frac{v(x, y)t(x_0, y_0)}{\sqrt{(x - x_0)^2 + (y - y_0)^2}}\,dxdx_0\right]dydy_0. \quad (19)$$

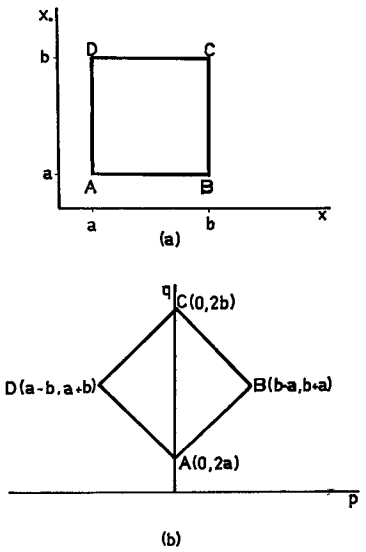

Fig. 4. (a) Region under consideration in x–x_0 plane. (b) Transformed region in the p–q plane.

Now perform the transformation $x-x_0=p$ and $x+x_0=q$ as suggested for the logarithmic singularity [9]. Referring to Fig. 4(a) and (b) and using the symmetry in Fig. 4(b), l_1 may be written as

$$l_1 = \int_{y_0=c}^{d}\int_{y=c}^{d}\left[\frac{1}{2}\int_{p=0}^{b-a}\int_{q=2a+p}^{2b-p}\frac{v\left(\frac{p+q}{2}, y\right)t\left(\frac{-p+q}{2}, y_0\right)+v\left(\frac{-p+q}{2}, y\right)t\left(\frac{p+q}{2}, y_0\right)}{\sqrt{p^2+(y-y_0)^2}}\,dqdp\right] \cdot dydy_0. \quad (20)$$

A similar procedure can now be repeated in the y–y_0 plane to yield

$$l_1 = \frac{1}{4}\int_{p=0}^{b-a}\int_{r=0}^{d-c}\frac{1}{\sqrt{p^2+r^2}} \cdot \int_{q=2a+p}^{2b-p}\int_{s=2c+r}^{2d-r} F(p, r, q, s)\,dsdqdrdp \quad (21)$$

where

$$\begin{aligned} F(p,r,q,s) = {} & v\left(\frac{p+q}{2}, \frac{r+s}{2}\right)t\left(\frac{-p+q}{2}, \frac{-r+s}{2}\right) \\ & + v\left(\frac{-p+q}{2}, \frac{r+s}{2}\right)t\left(\frac{p+q}{2}, \frac{-r+s}{2}\right) \\ & + v\left(\frac{p+q}{2}, \frac{-r+s}{2}\right)t\left(\frac{-p+q}{2}, \frac{r+s}{2}\right) \\ & + v\left(\frac{-p+q}{2}, \frac{-r+s}{2}\right)t\left(\frac{p+q}{2}, \frac{r+s}{2}\right). \end{aligned} \quad (22)$$

The integration indicated by (21) can be performed if the following integrals can be evaluated:

$$l_1 = \int_{p=0}^{b-a}\int_{r=0}^{d-c}\frac{H(p, r)}{\sqrt{p^2+r^2}}\,drdp \quad (23)$$

where

$$H(p, r) = \int_{q=2a+p}^{2b-p}\int_{s=2c+r}^{2d-r} F(p, r, q, s)\,dsdq. \quad (24)$$

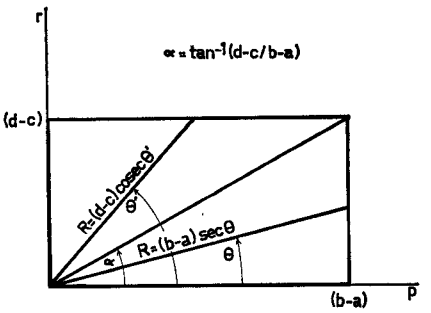

Fig. 5. Regions of integration for (26).

The integral in (23) can be evaluated by performing the transformation

$$\begin{aligned} p &= R\cos\theta \\ r &= R\sin\theta \end{aligned} \quad (25)$$

and, referring to Fig. 5,

$$\begin{aligned} l_1 = {} & \int_{\theta=0}^{\alpha}\int_{R=0}^{(b-a)\sec\theta}\frac{H(R,\theta)}{R}\,RdRd\theta \\ & + \int_{\theta=\alpha}^{\pi/2}\int_{R=0}^{(d-c)\csc\theta}\frac{H(R,\theta)}{R}\,RdRd\theta. \end{aligned} \quad (26)$$

Note that in (26) the singularity is no longer present. Each integral in (26) can be evaluated using a Cartesian product of Gaussian quadrature formulas in the R–θ plane. Once the quadrature nodes for (26) are obtained (24) becomes a definite integral that can be evaluated by a Cartesian product rule in the s–q plane.

The third case to be considered is a pseudosingularity that takes the form

$$l_2 = \int_{y_0=c}^{d}\int_{x_0=a}^{b}\int_{y=c}^{d}\int_{x=a}^{b}\frac{v(x, y)t(x_0, y_0)}{\sqrt{k^2+(x-x_0)^2+(y-y_0)^2}} \cdot dxdydx_0dy_0. \quad (27)$$

The integrand here is in fact continuous throughout the region of integration, but has very large derivatives as well as values if k is small; straightforward use of Gauss–Legendre quadratures therefore leads to bounded but very large error. From the numerical point of view, this integral is difficult and requires special treatment similar to true singular integrals. This problem is handled much the same way as the above singularity. In this case, the equation equivalent to (23) is of the form

$$l_2 = \int_{p=0}^{b-a}\int_{r=0}^{d-c}\frac{H(p, r)}{\sqrt{k^2+p^2+r^2}}\,drdp. \quad (28)$$

After performing the transformation given in (25)

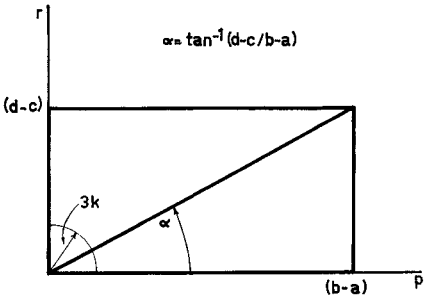

Fig. 6. Regions of integration for (29).

and referring to Fig. 6, l_2 may be written as

$$l_2 = \int_{\vartheta=0}^{\pi/2} \int_{R=0}^{3k} \frac{RH(R,\theta)}{\sqrt{k^2+R^2}}\, dRd\theta + \int_{\vartheta=0}^{\alpha} \int_{R=3k}^{(b-a)\sec\theta} \frac{RH(R,\theta)}{\sqrt{k^2+R^2}}\, dRd\theta + \int_{\theta=\alpha}^{\pi/2} \int_{R=3k}^{(d-c)\csc\theta} \frac{RH(R,\theta)}{\sqrt{k^2+R^2}}\, dRd\theta. \quad (29)$$

To evaluate the first integral in (29), a one-dimensional weighted Gaussian formula was developed with $R/\sqrt{k^2+R^2}$ as the weight. This ensures that the pseudo-singular part of the integral is evaluated rather accurately. The second and third integrals in (29) are nonsingular, and straightforward Cartesian products were taken.

Results

A sufficiently large number of computations has been carried out using the above method to permit determining, within a small percentage error, the static capacitance of any rectangular plate pair separated by an infinite dielectric sheet (or, what is equivalent, of any rectangular plate separated by a dielectric sheet from an infinite conducting sheet). The results of these calculations are given in Figs. 7–12.

In Fig. 7, results comparable to those of Reitan [1], Harrington [2], or Farrar and Adams [4], but considerably more extensive, are shown for two parallel plates *in vacuo*. The plates are taken to be thin, of width w, length l, and separated by a distance d. It will be noted that the range of w/l shown thus covers all possible cases: $w/l=0$ corresponds to infinitely long parallel strips, while $w/l=1$ represents a pair of square plates. Cases with $w/l>1$ are not excluded, since it is only necessary to exchange the labeling of the width w and length l. The parameter in Fig. 7, d/w, has been used in preference to d/l for two reasons. First, this choice makes the left-hand endpoints ($w/l=0$) of all curves represent strip pairs of a specified width-separation ratio, directly comparable with the microstrip computations given earlier [6]. Secondly, it has been found that Figs. 8–12 are rendered most easily legible by this choice. The capacitance values themselves have been normalized to the capacitance of a similar pair of plates,

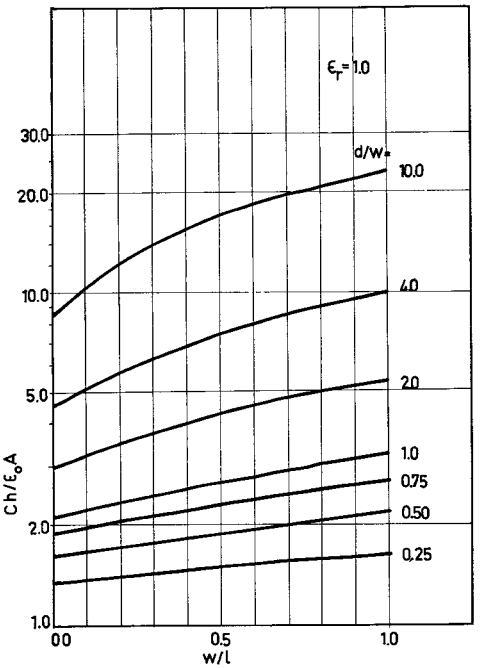

Fig. 7. Normalized capacitance against ground plane $Ch/\epsilon_0 A$ versus plate width-to-length ratio w/l for plate spacing-to-width ratios $d/w=10.0$, 4.0, 2.0, 1.0, 0.75, 0.5, and 0.25 and relative dielectric constant $\epsilon_r=1.0$.

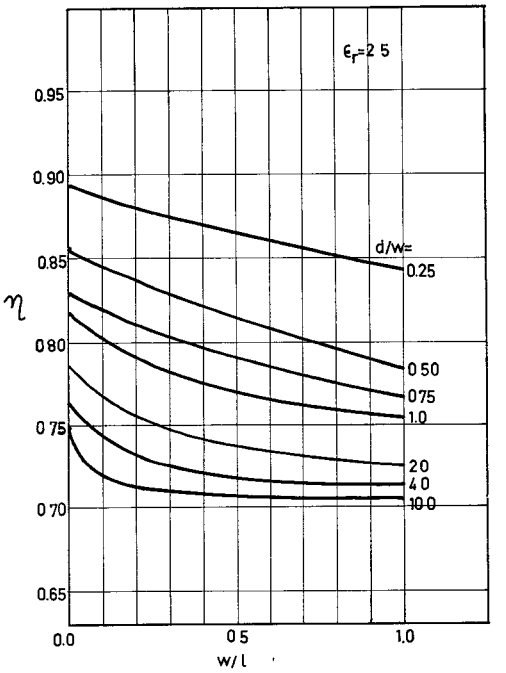

Fig. 8. Effective filling factor η versus width-to-length ratio w/l for plate spacing-to-width ratios $d/w=10.0$, 4.0, 2.0, 1.0, 0.75, 0.5, 0.25 and relative dielectric constant $\epsilon_r=2.5$.

calculated on the assumption that the electric flux lines pass straight across from plate to plate (the "infinite parallel plate" assumption).

If a dielectric sheet of relative permittivity ϵ_r is inserted between the parallel plates, the capacitance rises from its original free-space value C_0 to some higher value C. This value, however, is always lower than the value C_r that would be achieved by filling all space with

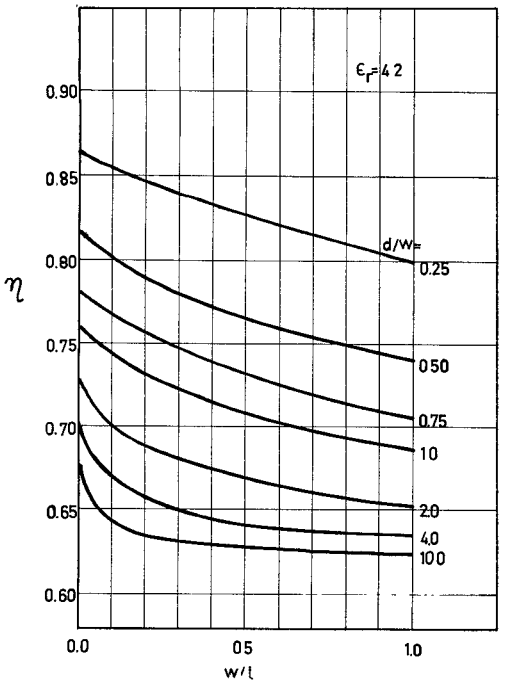

Fig. 9. Same as Fig. 8 with $\epsilon_r = 4.2$.

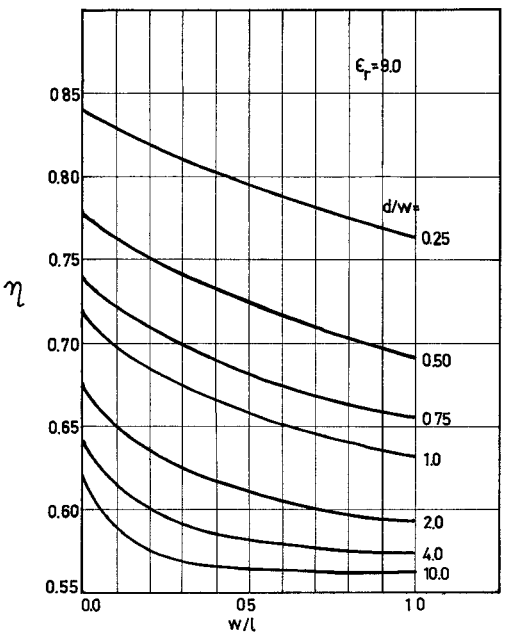

Fig. 10. Same as Fig. 8 with $\epsilon_r = 9.0$.

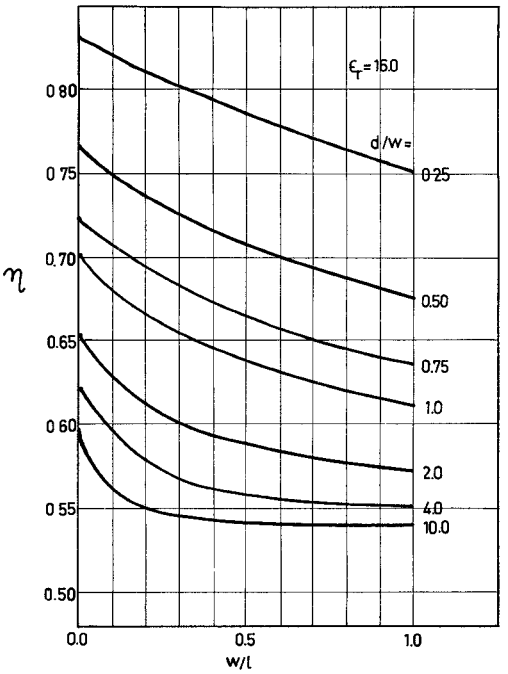

Fig. 11. Same as Fig. 8 with $\epsilon_r = 16.0$.

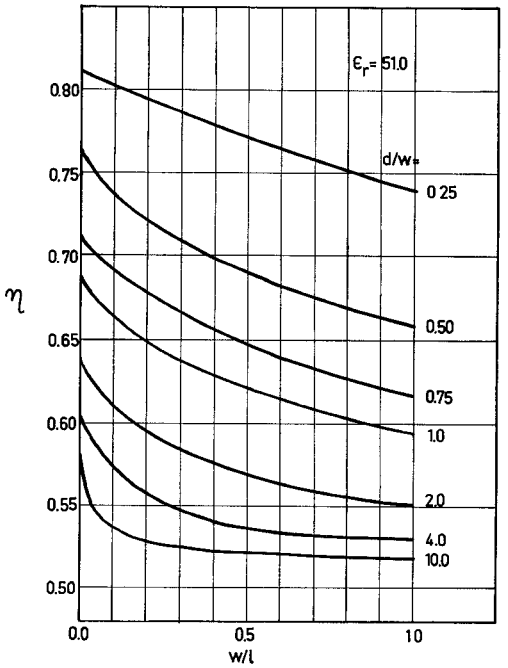

Fig. 12. Same as Fig. 8 with $\epsilon_r = 51.0$.

dielectric of permittivity ϵ_r. One may define *effective filling factor* η as the ratio of capacitance with dielectric sheet in place to capacitance obtained in a space of homogeneous relative permittivity ϵ_r:

$$\eta = C/C_r. \tag{30}$$

Since $C_r = \epsilon_r C_0$, the actual capacitance C can be found from

$$C = \eta \epsilon_r C_0 \tag{31}$$

provided η is known.

Values of the effective filling factor η are given in Figs. 8–12 for $\epsilon_r = 2.5$, 4.2, 9, 16, 51; these choices are appropriate to some of the commonly employed dielectric materials. While η is obviously dependent on ϵ_r, as well as on the geometric parameters, its variation with ϵ_r is not very rapid. Therefore, very little accuracy is lost by, for example, using Fig. 11 for all $14 \leq \epsilon_r \leq 18$ without modification or correction.

If capacitance values are required for relative permittivities not close to one of the tabulated values,

linear interpolation has been found quite effective. As an extreme example, suppose $w/l=0.4$, $d/w=0.5$, and $\epsilon_r=4.2$. Using Fig. 9 one obtains $\eta=0.772$. Were this curve not available, it would be necessary to interpolate between Fig. 8 (from which $\eta=0.822$) and Fig. 10 ($\eta=0.731$). The interpolation yields $\eta=0.798$ in error by less than four percent, despite the very large range of relative permittivities spanned by the interpolation. Various numerical tests have shown that interpolation between adjacent pairs of computed curves ordinarily yields errors of about one percent and occasionally two percent. It is believed that this accuracy level is entirely adequate for practical work, where neither permittivities nor geometric parameters are likely to be known much more accurately.

Experimental measurements were performed on five rectangular plates on a dielectric substrate of $\epsilon_r=3.26$. The results agree with the calculated values to within the experimental error.

Conclusion

A new projective method has been presented in this paper for the calculation of self and mutual capacitances of flat conductor sections attached to dielectric substrates. The computing times achievable by this method have been found sufficiently short to permit presentation of a set of universal curves, from which the capacitance of a pair of rectangular plates separated by a dielectric sheet or of a single plate on a conductively backed substrate may be found within a few percent. The method itself is capable of substantially wider application and will be used in the future for solving a variety of other related problems.

Acknowledgment

The authors wish to thank Dr. A. Gopinath, Z. Csendes, and other colleagues for their helpful discussions and assistance. They also wish to thank Mrs. P. Hyland for typing the manuscript and A. White for preparing the figures.

References

[1] D. K. Reitan, "Accurate determination of the capacitance of rectangular parallel-plate capacitors," *J. Appl. Phys.*, vol. 30, no. 2, pp. 172–176, Feb. 1959.
[2] R. F. Harrington, *Field Computation by Moment Methods*. New York: Macmillan, 1968.
[3] A. T. Adams and J. R. Mautz, "Computer solution of electrostatic problems by matrix inversion," in *Proc. 1969 Nat. Electronics Conf.*, pp. 198–201.
[4] A. Farrar and A. T. Adams, "Computation of lumped microstrip capacities by matrix methods—Rectangular sections," *IEEE Trans. Microwave Theory Tech.* (Corresp.), vol. MTT-19, pp. 495–496, May 1971.
[5] I. Stakgold, *Boundary Value Problems of Mathematical Physics*, vol. II. New York: Macmillan, 1968.
[6] P. Silvester, "TEM wave properties of microwave transmission lines," *Proc. Inst. Elec. Eng.*, vol. 115, no. 1, pp. 43–48, Jan. 1968.
[7] P. D. Patel, "Calculation of capacitance coefficients for a system of irregular finite conductors on a dielectric sheet," *IEEE Trans. Microwave Theory Tech.*, vol. MTT-19, pp. 862–869, Nov. 1971.
[8] P. J. Davis and P. Rabinowitz, *Numerical Integration*. Waltham, Mass.: Blaisdell, 1967.
[9] P. Silvester and M.-S. Hsieh, "Projective solution of integral equations arising in electric and magnetic field problems," *J. Comput. Phys.*, vol. 8, 1971.
[10] S. G. Mikhlin and K. L. Smolitskiy, *Approximate Methods for Solution of Differential and Integral Equations*. New York: American Elsevier, 1967.